Chapter 1

Detection of dark spins via cross-relaxations

In this chapter, we will see how...

1.1 Flip-Flops, double flips and cross-relaxation

The dominant form of interaction between two distant spins is the magnetic dipole-dipole interaction. For two spins with with vector spin Hamiltonian $\hat{\mathbf{S}}_1$ and $\hat{\mathbf{S}}_2$, separated by a distance $\mathbf{r} = r\mathbf{u}$, the dipole-dipole interaction Hamiltonian reads (see Appendix A) :

$$\mathcal{H}_{dd} = \frac{J_0}{r^3} \left[\hat{\mathbf{S}}_1 \cdot \hat{\mathbf{S}}_2 - 3(\hat{\mathbf{S}}_1 \cdot \mathbf{u})(\hat{\mathbf{S}}_2 \cdot \mathbf{u}) \right], \tag{1.1}$$

where $J_0 = \frac{\mu_0 \gamma_1 \gamma_2 \hbar^2}{4\pi}$. For two electronic spins with $g-$factors close to 2 (which is the case for the NV center and most spin defect in diamond), the numerical value of J_0 is $(2\pi)\, 52$ MHz $\cdot$ nm^3.

Flip-flop, in the context of dipole-dipole interaction, is the mechanism which exchanges a quantum of spin between two spins. For an initial state of two spins
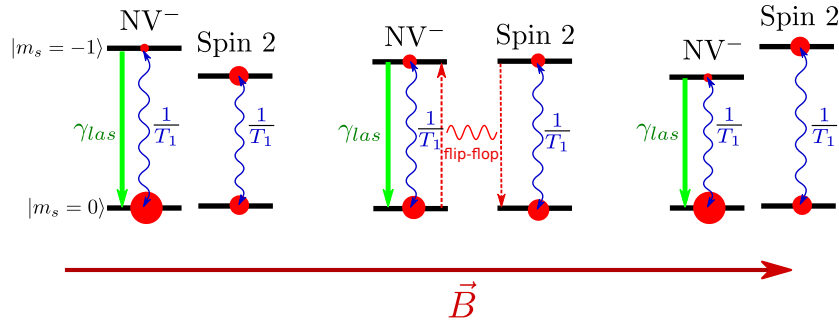

Figure 1.1: Illustration of cross-relaxations between an NV center and an unpolarized spin. Red dots represent the population in each states, and the arrows the various population transfer mechanisms

$\left|m_s^1 = i; m_s^2 = j\right\rangle$, a flip-flop process will result in a final state $|i+1; j-1\rangle$ or $|i-1; j+1\rangle$. The effective rate of this process depends on the matrix element $\langle i; j|\mathcal{H}_{dd}|i\pm1; j\mp1\rangle$, as well as the resonance condition between the initial and final state. We should note that for two identical spins, the flip-flop process $|i; i\pm1\rangle\langle i\pm1, i|$ is always resonant.

Another mechanism authorized by the dipole-dipole Hamiltonian is the double-flip, either up or down, which couple the states $|i; j\rangle$ and $|i-1; j-1\rangle$ or $|i+1; j+1\rangle$. For a single spin species in a strong magnetic field, the lift of the various spin levels by the Zeeman effect means that no double-flip process can be resonant. However with weak magnetic field or when two different spin species are present, double flip process can be as important as flip-flops since the matrix elements $\langle i; j|\mathcal{H}_{dd}|i\pm1; j\pm1\rangle$ are typically of the same order of magnitude as the flip-flop ones.

Cross-relaxation (CR) is the transfer of polarization from one spin to another (or more generally from one family of spins to another family). This process con occur either through flip-flops, or through double flips, as long as the resonance condition between the two spins is met.

Fig. 1.1 illustrates CR between a polarized NV center and an unpolarized second spin. When the two considered spin transitions become resonant, in this case by tuning a magnetic field, polarization from the NV center will be transferred to the second spin, meaning in this case that the NV center will end up less polarized and the second spin more polarized.

The reason why CR tend to depolarize the NV center simply comes from a rate equation : since the initial NV population is higher in the $|0\rangle$ state than in the $|-1\rangle$ state, the flip-flop (or double flip) process that makes the NV center go to $|-1\rangle$ (symbolized by the two red arrows in Fig. 1.1) is more likely than the reverse flip-flop. If we only focus on the NV center, cross-relaxation is simply another thermalization process due to the coupling of the NV center to its environment.

If we make the assumption that the spin bath coupled to the NV centers is Markovian, meaning that the dynamics of the bath is not affected by its coupling to the NV centers, we can then compute the modification in the NV relaxation rate $\Gamma_1 = \frac{1}{T_1}$ due to its coupling to Spin 2 [1]:

$$\delta\Gamma_1 = \frac{\Omega^2}{\Gamma_2^*} \frac{(\Gamma_2^*)^2}{(\delta\nu)^2 + (\Gamma_2^*)^2}, \tag{1.2}$$

where $\Omega = \frac{\langle i;j|\mathcal{H}_{dd}|j;i\rangle}{\hbar}$ is the matrix element of the dipole-dipole Hamiltonian that couples the initial and final states, $\Gamma_2^* = \frac{1}{T_2^*(\text{NV})} + \frac{1}{T_2^*(\text{Spin2})}$ is the joint dephasing rate of the NV center and the second spin, and $\delta\nu$ is the detuning between the central frequencies of the NV center and spin 2.

1.2   Dark spins in diamond

We refer by dark spins to spin defects which do not interact with light, which in the case of diamond defects consist of every known spin defect bar the NV center and the more recently found ST1 center [2, 3].

1.2.1   P1 centers and ^{13}C

By far the most common spin defects in NV-rich diamond, outside of NV centers, are the substitutional nitrogen centers N_S^0 known as the P1 centers, which have an electronic spin 1/2 and a nuclear spin 1, and the ^{13}C 1/2 nuclear spin which is present at 1.1% in natural abundance carbon, the remaining carbon atoms being almost exclusively the spinless ^{12}C isotope.

In NV-rich diamonds, these two impurities are the main causes of the inhomogeneous dephasing rate $\Gamma_2^* = 1/T_2^*$ of the NV centers ensemble [4]. The dephasing comes from the distribution of dipole-dipole coupling from each NV centers to its neighboring spin defects, which varies in space and time.

The dephasing rate caused by a given impurity is directly proportional to the diagonal dipole-dipole matrix elements [5]:

$$\Gamma_2^*(P1) \propto \Omega_{\mathrm{NV-P1}} = \frac{1}{\hbar}\sqrt{\sum_j |\langle NV=i; P1=j|\mathcal{H}_{\mathrm{dd}}|NV=i; P1=j\rangle|^2}. \quad (1.3)$$

Since the dipole-dipole coupling rate scales as $1/r^3$, and the distance r between each spin scales as the inverse cubic root of the concentration, it is expected that the dephasing rate associated with a particular impurity scales linearly with the concentration of the impurity. In the case of P1 centers, this was verified experimentally by [5] who found a value of $\Gamma_2^*(P1) = (2\pi)16$ kHz/ppm.

^{13}C is much more abundant than P1 center ($\sim 10\,000$ ppm at natural abundance) but being a nuclear spin, it has a gyromagnetic ratio $\approx 2.8\,10^3$ times smaller than that of the P1. This results in a contribution to $\Gamma_2^* \sim 10^3$ times smaller per impurity. It was found experimentally that the broadening caused by ^{13}C is $\Gamma_2^*(^{13}C) \approx 16$ Hz/ppm [6, 4]. For natural abundance diamond, this means that $\Gamma_2^*(^{13}C) \approx 160$ kHz.

1.2.2   Other spin defects, VH$^-$, War1

Other spin defects are also commonly found in diamond containing NV centers, such as charged vacancy or vacancy clusters [7], other nitrogen related defects [8], transition metals [9], and especially for CVD grown diamond, hydrogen related defects [10], since the CVD plasma contains up to 95 % hydrogen.

Of particular interest in this chapter are two defects: the VH$^-$ defect [11, 12] and the War1 defect [13].

The VH$^-$ defect, prior to our observations, had only been observed *via* electron paramagnetic resonance (EPR) in CVD grown diamond. It is formed by a vacancy with a hydrogen atom bonded to one of the four dangling carbon bond, with an extra electron trapped in the vacancy. This defect has a similar electronic structure to the NV$^-$ which results in an electronic spin-1 with a similar zero field splitting parameter (see Table [REF]). Although the presence of hydrogen in this defect was confirmed by isotopic study, it has been debated whether this defect was VH$^-$ or V$_2$H$^-$ due to a conflict with *ab initio* calculations [14]. The defect is therefore sometimes referred as V$_n$H$^-$. In this manuscript I will employ the original name VH$^-$.

The War1 defect, named after the University of Warwick where it was first observed in a CVD diamond [13], is another spin-1 defect whose chemical structure remains unknown. No hyperfine structure could be discerned in the rela-

tively broad EPR line, and the use of deuterium instead of ^{1}H did not change the shape of the line.

1.3   NV center relaxometry

1.3.1   Principle of NV center Relaxometry

Detection *via* cross-relaxation with NV centers fall under the more general technique of NV relaxometry, where we are effectively measuring a modification in the NV center spin lifetime T_1. Relaxometry with NV centers has been used not only to measure resonant cross-relaxation with dark spins [**hall2016detection** , 15, 16, 17, 18, 19, 20, 21, 22], but also to probe the magnetic noise in the diamond environment coming from spins [23], ions[24], free radicals [25], magnetic domains [26]...

There can be several advantages to use relaxometry protocols, which measures a change in the NV T_1, over the more common magnetometry protocols that rely on a change in the NV T_2 or T_2^*: the first and most obvious one is that relaxometry does not need to use an external microwave field. This however comes at the cost of a greater precision needed on the external magnetic field. Relaxometry also allows AC-magnetic field sensing in the GHz regime, where traditional microwave-based AC-megnetometry is limited to tens of MHz [27, 28]. Finally, relaxometry measurement can be more sensitive than the T2-based one in some instances [23], which comes from the fact that changes in NV T_1 times are easier to detect than changes in T_2 or T_2^* since T_1 is much longer than T_2 or T_2^*.
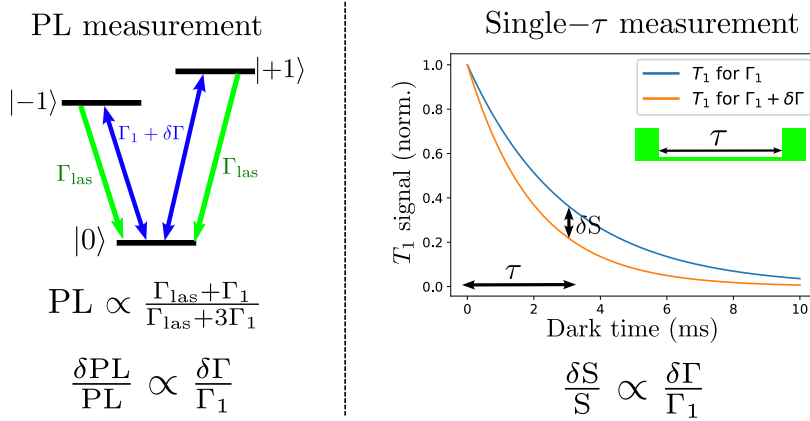
1.3.2   PL and single$-\tau$ relaxometry protocols

Figure 1.2: Representation of the two relaxometry protocol. Left : representation of the three level system of the NV center with the polarization rate Γ_{las} and spin decay rates $\Gamma_1 = 1/T_1$ and the perturbation $\delta\Gamma$. Right: simulation of a T_1 measurement for $1/\Gamma_1 = 3$ ms and $1/(\Gamma_1 + \delta\Gamma) = 2$ ms. δS represents the maximum difference in signal between the two curves for a dark time τ.

There are two ways to measure a change in the spin T_1, as represented on

Fig. 1.2. The first and most basic method simply consist in monitoring the PL of the NV centers : since the PL is proportional to the population in the $|0\rangle$ state, which itself results from an equilibrium between the polarization rate Γ_{las} and the spin decay rate $\Gamma_1 = 1/T_1$. A change in Γ_1 will therefore conduct to a new equilibrium with a different PL. For a small enough change $\delta\Gamma << \Gamma_1$, we can consider that we remain in the linear regime, hence why $\frac{\delta \text{PL}}{\text{PL}} \propto \frac{\delta\Gamma}{\Gamma_1}$.

The second method is a pulsed sequence referred as single$-\tau$ measurement, used for example in [29, 30, 31]. It simply consists in a T_1 measurement sequence (as seen in chapter 1) where you first polarize the spins in the $|0\rangle$ state with a laser pulse and read out the spin state with a second laser pulse after a dark time τ. In this case however, instead of scanning the time τ, you fix its value to maximize the sensitivity in a change of T_1 (typically $\tau \approx T_1$). Again, assuming you are in the linear regime, you observe a change in signal proportional to the change in Γ_1 : $\frac{\delta \text{S}}{\text{S}} \propto \frac{\delta\Gamma}{\Gamma_1}$.

It is argued in [26] that both methods result in similar signal to noise ratio: in the first case you need to adjust $\Gamma_{\text{las}} \sim \Gamma_1$ to maximize the PL contrast, meaning that the laser power used is very far from the saturation limit (typically $\Gamma_1 \approx 10^3$ s^{-1} and $\Gamma_{\text{sat}} = 5 \cdot 10^6$ s^{-1}[32]), while the second method needs to wait a time $\tau \sim T_1$ between each measurement, which result in a similar PL count and shot noise limit in both case.

On a technical level, the PL-based method is easier to implement since it does not require the use of a pulsed laser, and uses an overall smaller laser power, however it is more sensitive to drifts and changes in the optical setup. Most of the relaxometry measurement in this manuscript were performed using a PL-based detection.
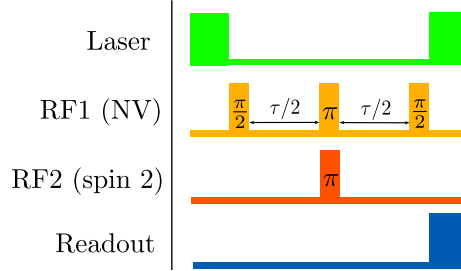
1.3.3 Comparison with DEER protocol

Figure 1.3: Pulse sequence of the DEER protocol

Outside of cross-relaxations, another protocol exists to address dark spin resonance with NV centers, based on a modification of the NV T_2 time [33]. This protocol called double electron-electron resonance (DEER) is depicted on Fig. 1.3. The pulse sequence consist in a spin-echo sequence on the NV center, as described in chapter 1, with a simultaneous $\pi-$pulse on the probed dark spins during the rephasing pulse on the NV centers. This additional pulse means that the static (or slowly variable) contribution of the probed spins to the T_2^* of the NV center wont be rephased. The newly measured T_2 time should therefore be slightly shorter:

$$\frac{1}{T_2^{\text{DEER}}} = \frac{1}{T_2^{\text{echo}}} + \delta\Gamma, \tag{1.4}$$

where $\delta\Gamma$ is the contribution of the dark spin to the T_2^* of the NV center through NV-dark spin dipole-dipole interaction.

By scanning the frequency of the second microwave (RF2) and monitoring the T_2 time of the NV centers, one can therefore find dark spin resonance without having to bring them to resonance with NV centers, which can be useful when the dark spin resonance is very far detuned from the NV one.

While both cross-relaxation and DEER measure the dipole-dipole coupling of dark spins to an NV center, there are several differences between the two protocols:

Frist, the two protocols do not measure the same elements of the dipole-dipole Hamiltonian: CR measures the off-diagonal elements $\Omega_{\text{CR}} = \langle i, j | \mathcal{H}_{\text{dd}} | j, i \rangle / \hbar$ which are responsible for the flip-flops or double flips, while DEER measures the diagonal elements $\Omega_{\text{DEER}} = \langle i, j | \mathcal{H}_{\text{dd}} | i, j \rangle / \hbar$ which are responsible for the pure dephasing. These terms however are on average of the same amplitude, and when averaging over an ensemble we can consider $\Omega_{\text{CR}} \sim \Omega_{\text{DEER}}$

Second and more importantly, the scaling is not the same in both cases : CR measures a change in the NV decay rate $\Gamma_1 = 1/T_1$ which is proportional to Ω_{CR}^2, as given by eq. 1.2, while DEER measures a change in $\Gamma_2 = 1/T_2$ which is proportional to Ω_{DEER}, as given by eq. 1.3. This means that the signal of CR scales quadratically with the impurity concentration, while the DEER signal scales linearly with it. CR is therefore more suited to probe concentrated impurities, when the average distance between the NV and the probed spin is small.
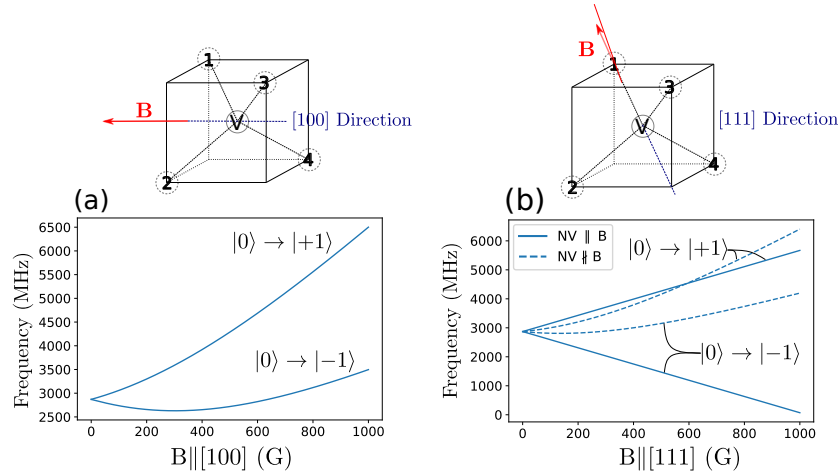
1.4   Choice of the B scan orientation

Figure 1.4: Label

Since relaxometry does not rely on a microwave field, the only parameter left to tune is the external magnetic field, which is often scanned with an electro-

magnet. Due to the strong NV anisotropy however, the direction along which **B** is scanned plays a crucial role in the ability to detect dark spins.

Fig. 1.4 shows the two main choices of scanning orientation : either **B** $\parallel$ [100]

1.5   Attribution of the VH$^-$ and War1 lines

Bibliography

[1] LT Hall et al. "Detection of nanoscale electron spin resonance spectra demonstrated using nitrogen-vacancy centre probes in diamond". In: *Nature communications* 7.1 (2016), pp. 1–9.

[2] Sang-Yun Lee et al. "Readout and control of a single nuclear spin with a metastable electron spin ancilla". In: *Nature nanotechnology* 8.7 (2013), pp. 487–492.

[3] Roger John et al. "Bright optical centre in diamond with narrow, highly polarised and nearly phonon-free fluorescence at room temperature". In: *New Journal of Physics* 19.5 (2017), p. 053008.

[4] John F Barry et al. "Sensitivity optimization for NV-diamond magnetometry". In: *Reviews of Modern Physics* 92.1 (2020), p. 015004.

[5] Erik Bauch et al. "Decoherence of ensembles of nitrogen-vacancy centers in diamond". In: *Physical Review B* 102.13 (2020), p. 134210.

[6] JA Van Wyk et al. "The dependences of ESR line widths and spin-spin relaxation times of single nitrogen defects on the concentration of nitrogen defects in diamond". In: *Journal of Physics D: Applied Physics* 30.12 (1997), p. 1790.

[7] LS Hounsome et al. "Origin of brown coloration in diamond". In: *Physical Review B* 73.12 (2006), p. 125203.

[8] ME Newton. "EPR, ENDOR and EPR Imaging of Defects in Diamond". In: *Electron Paramagnetic Resonance* 20 (2007), pp. 131–156.

[9] J Isoya et al. "Fourier-transform and continuous-wave EPR studies of nickel in synthetic diamond: Site and spin multiplicity". In: *Physical Review B* 41.7 (1990), p. 3905.

[10] Christopher Brett Hartland. "A study of point defects in CVD diamond using electron paramagnetic resonance and optical spectroscopy". PhD thesis. University of Warwick UK, 2014.

[11] Claire Glover et al. "Hydrogen incorporation in diamond: The nitrogen-vacancy-hydrogen complex". In: *Physical review letters* 90.18 (2003), p. 185507.

[12] Claire Glover et al. "Hydrogen incorporation in diamond: The vacancy-hydrogen complex". In: *Physical review letters* 92.13 (2004), p. 135502.

[13] Robin Cruddace. "Magnetic resonance and optical studies of point defects in single crystal CVD diamond". PhD thesis. University of Warwick, 2007.

[14] MJ Shaw et al. "Importance of quantum tunneling in vacancy-hydrogen complexes in diamond". In: *Physical review letters* 95.10 (2005), p. 105502.

[15] Eric van Oort and Max Glasbeek. "Cross-relaxation dynamics of optically excited N-V centers in diamond". In: *Physical Review B* 40.10 (1989), p. 6509.

[16] K Holliday et al. "Optical hole-bleaching by level anti-crossing and cross relaxation in the NV centre in diamond". In: *Journal of Physics: Condensed Matter* 1.39 (1989), p. 7093.

[17] Seiji Armstrong et al. "NV–NV electron–electron spin and NV–NS electron—electron and electron-nuclear spin interaction in diamond". In: *Physics Procedia* 3.4 (2010), pp. 1569–1575.

[18] RJ Epstein et al. "Anisotropic interactions of a single spin and dark-spin spectroscopy in diamond". In: *Nature physics* 1.2 (2005), pp. 94–98.

[19] Arne Wickenbrock et al. "Microwave-free magnetometry with nitrogen-vacancy centers in diamond". In: *Applied Physics Letters* 109.5 (2016), p. 053505.

[20] James DA Wood et al. "Wide-band nanoscale magnetic resonance spectroscopy using quantum relaxation of a single spin in diamond". In: *Physical Review B* 94.15 (2016), p. 155402.

[21] Nir Alfasi et al. "Detection of paramagnetic defects in diamond using off-resonance excitation of NV centers". In: *Physical Review B* 99.21 (2019), p. 214111.

[22] Reinis Lazda et al. "Cross-relaxation studies with optically detected magnetic resonances in nitrogen-vacancy centers in diamond in external magnetic field". In: *Physical Review B* 103.13 (2021), p. 134104.

[23] S Steinert et al. "Magnetic spin imaging under ambient conditions with sub-cellular resolution". In: *Nature communications* 4.1 (2013), pp. 1–6.

[24] J-P Tetienne et al. "Spin relaxometry of single nitrogen-vacancy defects in diamond nanocrystals for magnetic noise sensing". In: *Physical Review B* 87.23 (2013), p. 235436.

[25] Linyan Nie et al. "Quantum sensing of free radicals in primary human dendritic cells". In: *Nano letters* 22.4 (2021), pp. 1818–1825.

[26] Aurore Finco et al. "Imaging non-collinear antiferromagnetic textures via single spin relaxometry". In: *Nature communications* 12.1 (2021), pp. 1–6.

[27] Zhecheng Wang et al. "Picotesla magnetometry of microwave fields with diamond sensors". In: *arXiv preprint arXiv:2206.08533* (2022).

[28] Scott T Alsid et al. "A Solid-State Microwave Magnetometer with Picotesla-Level Sensitivity". In: *arXiv preprint arXiv:2206.15440* (2022).

[29] Matthew Pelliccione et al. "Two-dimensional nanoscale imaging of gadolinium spins via scanning probe relaxometry with a single spin in diamond". In: *Physical Review Applied* 2.5 (2014), p. 054014.

[30] Dominik Schmid-Lorch et al. "Relaxometry and dephasing imaging of superparamagnetic magnetite nanoparticles using a single qubit". In: *Nano letters* 15.8 (2015), pp. 4942–4947.

[31] Jean-Philippe Tetienne et al. "Scanning nanospin ensemble microscope for nanoscale magnetic and thermal imaging". In: *Nano Letters* 16.1 (2016), pp. 326–333.

[32] A Dréau et al. "Avoiding power broadening in optically detected magnetic resonance of single NV defects for enhanced dc magnetic field sensitivity". In: *Physical Review B* 84.19 (2011), p. 195204.

[33] Maksym Serbyn et al. "Interferometric probes of many-body localization". In: *Physical review letters* 113.14 (2014), p. 147204.